



OPEN ACCESS

Eurasian Journal of Analytical Chemistry

ISSN: 1306-3057

2017 12(7):977-986

DOI: 10.12973/ejac.2017.00226a



Corrosion Inhibition of X70 Steel by Butyl Quaternary Ammonium Halides Compounds in Sodium Chloride Solution

Hamdi Ahmed

Laboratoire Physico-Chimie des Matériaux (LPCM), Université Amar Telidji BP 37G 03000 Laghouat, ALGERIA

Bourzeg Mohamed Tahar

Laboratoire Physico-Chimie des Matériaux (LPCM), Université Amar Telidji BP 37G 03000 Laghouat, ALGERIA

Taouti Mohamed Ben Abdallah

Laboratoire Physico-Chimie des Matériaux (LPCM), Université Amar Telidji BP 37G 03000 Laghouat, ALGERIA

Benbortal Djamel

Laboratoire Physico-Chimie des Matériaux (LPCM), Université Amar Telidji BP 37G 03000 Laghouat, ALGERIA

Received 12 December 2016 • Revised 28 March 2017 • Accepted 29 March 2017

ABSTRACT

This study investigates corrosion inhibition of X70 steel surfaces, by Butyl-Quaternary-Ammonium halides, in a 3% of NaCl solution with pH = 6. In the first part, the influence of inhibitor concentration study reveals that the I-TBA is the best inhibitor ($\approx 79\%$ on the X70 steel). Each compounds exhibits Langmuirian behaviour and the values of ΔG° indicate that we have a physical adsorption. In the second part, the influence of immersion time study on the stability of the formed films reveals that they are stable and require about 150 min to be established, and deliver efficiencies that overtake the 70% in all cases. The stationary polarization curves and electrochemical impedance spectroscopy (EIS) diagrams show the high inhibitory effect of iodide compared with other halides.

Keywords: corrosion, inhibition, Butyl-Quaternary-Ammonium halides, X70 steel

INTRODUCTION

Mild steel is widely applied as constructional material in petrochemical industries due to its excellent mechanical properties and low cost. The breakdown of passive oxide films by aggressive anions such as Cl^- is frequently responsible for the failure of iron alloys in aqueous chloride solutions [1]. Organic nitrogen-based compounds such as amines and their salts have been used successfully as corrosion inhibitors in oilfield systems. In previous work, the mode of action of some amines to protect metals and alloys has been studied [2-9]. These compounds adsorb on the metal surface and suppress metal dissolution and reduction reactions. D.P

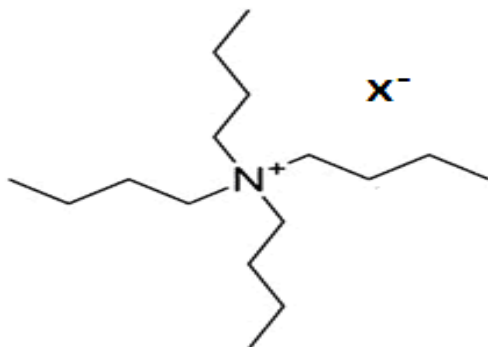
© **Authors.** Terms and conditions of Creative Commons Attribution 4.0 International (CC BY 4.0) apply.

Correspondence: Hamdi Ahmed, *Laboratoire Physico-Chimie des Matériaux (LPCM), Université Amar Telidji BP 37G 03000 Laghouat, Algeria.*

✉ ah.hamdi@lagh-univ.dz

Table 1. Chemical components of the X70 steel used in the tests

Element	Cr	Ni	Mn	Si	Nb	Co	Mo	Cu
(Wt %)	0.005	0.062	1.664	0.021	0.032	0.0159	0.0123	0.3152
Element	S	P	Ti	Al	C	V	Fe	
(Wt %)	0.001	0.009	0.003	0.034	0.172	0.0665	rest	

**Figure 1.** Chemical structure of X-TBA

Schweinsberg et al [10] found that the action of n-alkyl quaternary ammonium iodides is caused by the alkyl chain and this is attributed to van der Waals' forces. Other researchers [11-12] have also studied the structure of alkyl groups and the types of halide ions of alkyl quaternary ammonium halides inhibitors greatly influence the inhibition efficiency. In this paper the effect of butyl quaternary ammonium halides for two steel X70 corrosion in 3% NaCl has been investigated using Tafel method and electrochemical impedance spectroscopy (EIS).

EXPERIMENTAL

The material tested in this study is the low alloy X70 mild steel. The chemical composition of the material is given in [Table 1](#).

The test media were 500 ml, 3 wt% NaCl prepared from reagent grade chemicals and bi-distilled water. When needed, HCl or NaOH, were added to adjust the pH which is monitored with a pH/temperature (°C) meter. All experiments were conducted at pH = 6. The chemical structure of X-TBA is given in [Figure 1](#), where X is F, Cl, Br and I.

Potentiodynamic polarization measurements

For polarization studies, the X70 steel specimen was embedded in PVC holder using epoxy resin with an exposed area of 1.0 cm² as a working electrode. A platinum foil was used as a counter electrode. The reference electrode was a saturated calomel electrode (SCE) coupled to a Luggin capillary whose tip was located between the working electrode and the counter electrode. Before measurement, the electrode was immersed in a test solution at open circuit potential for 30 min until a steady state was reached. All polarization measurements were performed using TACUSSEL model PGP201 galvanostat / potentiostat corrosion

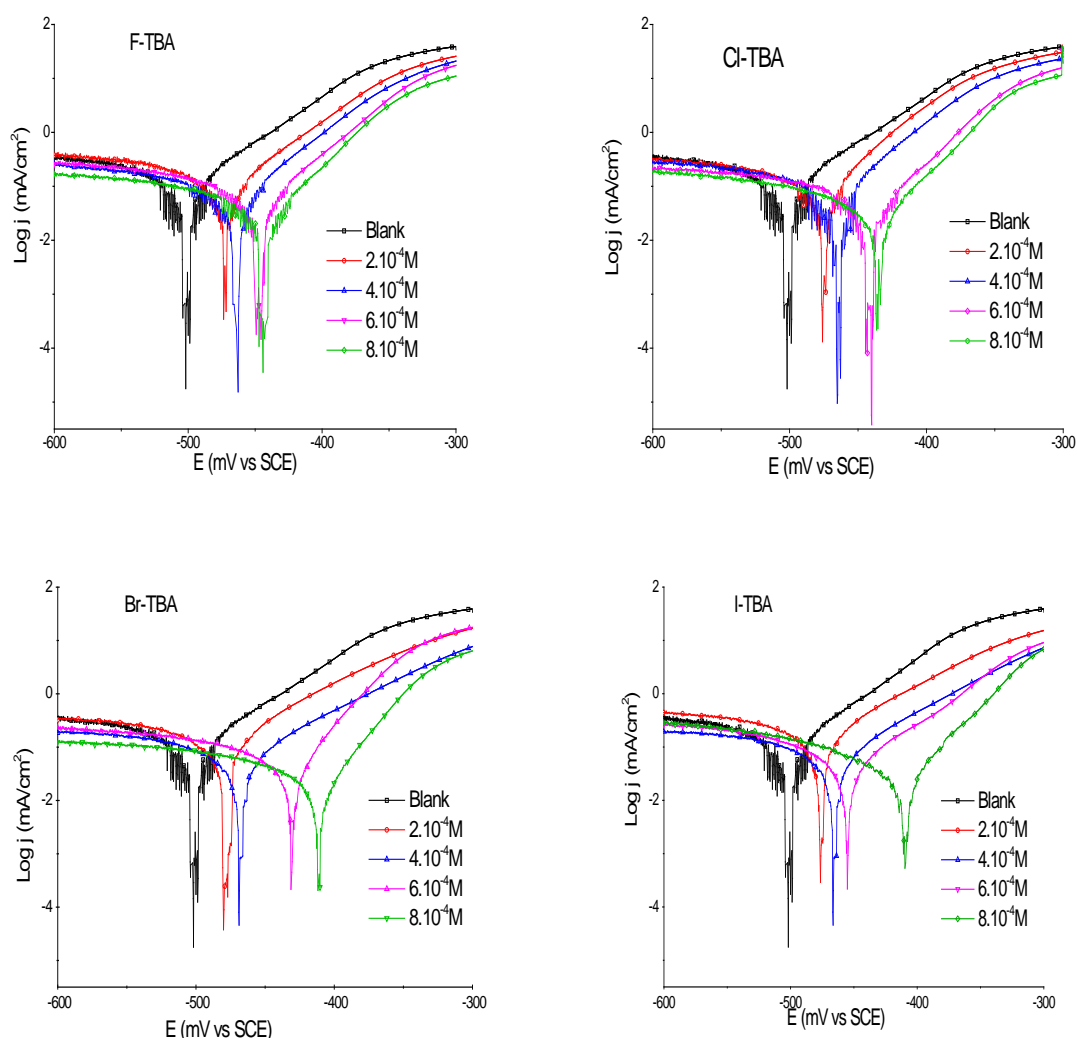


Figure 2. Polarization curves obtained from the X70 steel immersed in the solution without and with different concentrations of X-TBA

measurement system at room temperature under aerated conditions, the scanning rate was 0.5mVs^{-1} and a sweep range from an initial potential of -1000 mV/SCE to a final potential of $+200\text{ mV/SCE}$.

EIS measurements

The electrochemical impedance spectroscopy measurements were carried out using AC signals of amplitude 10 mV peak to peak at open circuit potential in the frequency range from 10 kHz to 10 mHz , using TACUSSEL model PGZ401 at room temperature in an aerated solution, a three-electrode cell has been used as in potentiodynamic polarization curves. The working electrode has been prepared from a cylindrical rod of X70 steel to get an area exposed

Table 2. Electrochemical parameters and inhibition efficiency at different inhibitors concentrations of X70 steel in 3%NaCl

Concentration (mol/L)	j_{corr} (mA/cm ²)	E_{corr} (mV/ECS)	β_a (mV/Dec)	R_p (Ω /cm ²)	V_{corr} (mm/an)	IE (%)	
Blank	0.1098	-505	95	251.8	1.202	/	
F-TBA	2.10 ⁻⁴	0.0793	-476	82	302.4	27.78	
	4.10 ⁻⁴	0.0542	-474	88	363.7	50.64	
	6.10 ⁻⁴	0.0495	-457	72	335.5	54.92	
	8.10 ⁻⁴	0.0362	-411	78	510.9	67.03	
	2.10 ⁻⁴	0.0749	-473	78	190.1	0.892	31.79
Cl-TBA	4.10 ⁻⁴	0.0529	-466	84	343.2	0.549	51.82
	6.10 ⁻⁴	0.0456	-445	70	281.3	0.434	58.47
	8.10 ⁻⁴	0.0313	-436	68	456.7	0.381	71.49
	2.10 ⁻⁴	0.0727	-488	82	105.0	1.003	33.79
Br-TBA	4.10 ⁻⁴	0.0516	-480	77	363.7	0.748	53.01
	6.10 ⁻⁴	0.0431	-432	87	336.2	0.504	60.75
	8.10 ⁻⁴	0.0305	-412	72	248.9	0.356	72.22
	2.10 ⁻⁴	0.0708	-475	46	178.99	0.870	35.52
I-TBA	4.10 ⁻⁴	0.0498	-465	46	362.1	0.797	54.64
	6.10 ⁻⁴	0.0366	-441	41	539.4	0.381	66.67
	8.10 ⁻⁴	0.0241	-435	37	227.4	0.281	78.05

to solution of 1 cm², and immersed in the test solution for different times, to establish a steady state open circuit potential. EIS is recorded at open circuit potentials.

The charge transfer resistance values were obtained from the diameter of the semi circles of the Nyquist plots.

RESULTS AND DISCUSSION

The study of the inhibition of corrosion of X70 steel with different concentrations of X-TB:

The polarization curves of X70 steel in 3% NaCl in the presence of various concentrations of X-TBA are shown in **Figure 2**. **Table 2** illustrates the corresponding electrochemical parameters. The inhibition efficiency was calculated using the following equation:

$$IE(\%) = 100 \times \frac{j_{corr} - j'_{corr}}{j_{corr}} \quad (1)$$

where j_{corr} and j'_{corr} are corrosion current densities without and with the inhibitor, respectively.

The inhibition efficiency increases with the presence of X-TBA. As can be found, with the increase of the halide ions F⁻, Cl⁻, Br⁻ and I⁻ corresponding to inhibitor F-TBA, Cl-TBA, Br-TBA and I-TBA respectively, the four compounds showed an acceptable performance, giving inhibition efficiency higher than 79 %, even at a very low concentration.

The inhibition efficiency of them follows the order F-TBA < Cl-TBA < Br-TBA < I-TBA, at high concentrations of all inhibitors, the values of cathodic slopes (β_c) remain substantially unchanged. The reduction mechanism is not affected by the presence of these inhibitors.

In **Table 2**, j_{corr} is the corrosion current density, E_{corr} the corrosion potential, β_a the anodic Tafel slope, R_p the polarisation resistance and V_{corr} the corrosion rate.

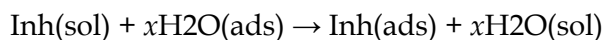
All the potential values are related to saturated calomel electrode (SCE)

The current densities on the anodic polarization curve were significantly reduced as inhibitor concentration is increased. The X-TBA is adsorbed at the anodic sites, since the diffusion limiting current of H^+ ions does not change with the application of inhibitor while the anodic reaction is greatly affected.

As it can be noted that the values of the polarization resistance are not increasing, this is due to the change in the values of the Tafel slopes.

Adsorption Isotherm at T=298 K

The adsorption of organic inhibitors at the metal/solution interface takes place through the replacement of water molecules by organic inhibitor molecules. According to the following process [13].



Values of surface coverage (θ) equation (2) corresponding to different concentrations of X-TBA, were calculated using the Potentiodynamic polarization measurements at 298 K after 30 mn of immersion and were used to determine which isotherm best described the adsorption process. However, the best agreement was obtained using the Langmuir adsorption isothermal equation (3) as follows:

$$\theta = \frac{j_{corr} - j'_{corr}}{j_{corr}} \quad (2)$$

$$\frac{C_i}{\theta} = \frac{1}{K_{ads}} + C_i \quad (3)$$

where C_i is the concentration of inhibitor and K_{ads} the adsorptive equilibrium constant.

Plots of C_i/θ against C_i yield straight lines as shown in **Figure 3**, and the linear regression parameters are listed in **Table 3** Both linear correlation coefficient (r) and slope are close to 1, indicating that the adsorption of the investigated inhibitors on the steel surface obeys the Langmuir adsorption. K_{ads} is related to the standard free energy of adsorption ΔG_{ads} as shown in the following equation [14]:

$$K_{ads} = \frac{1}{55.5} \exp\left(\frac{-\Delta G_{ads}}{RT}\right) \quad (4)$$

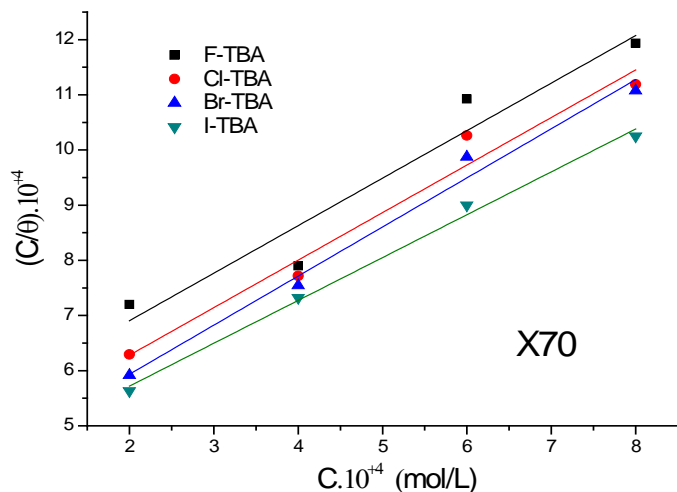


Figure 3. Curve fitting the corrosion of X70 steel in 3% NaCl in presence of different concentrations of X-TBA to Langmuir adsorption isotherm at 25°C

Table 3. Adsorption equilibrium constant (K_{ads}) and standard free energy of adsorption (ΔG_{ads}) of the investigated surfactants for X70 steel in a 3% NaCl solution at 25°C

Inhibitors	Correlation Coef.	Intercept $\times 10^4$	Slope	K_{ads}/M^{-1}	$\Delta G_{ads}/kJ.mol^{-1}$
F-TBA	0.77	7.4	0.68	913.70	-26.83
Cl-TBA	0.94	5.3	0.87	1646.84	-28.29
Br-TBA	0.92	5.69	0.76	1339.83	-27.78
I-TBA	0.99	4.57	0.77	1681.43	-28.34

Values of ΔG_{ads} up to -20 kJ/mol are consistent with the electrostatic interaction between the charged molecules and the charged metal (physical adsorption), while those more negative than -40 kJ/mol involve sharing or transfer of electrons from the inhibitor molecules to the metal surface to form a coordinate type of bond (chemisorption) [15,16].

The values of ΔG_{ads} of the two compounds presented in **Table 3** are located in a range between a -26.83 and 28.34 kJ/mol and this indicates physical adsorption. In addition to electrostatic interaction, there may be some other interactions.

Electrochemical impedance technique

Before testing the effect of the inhibitor by the EIS method, we optimize the immersion time without inhibitors. **Figure 4** show the results EIS tests performed respectively with X70 steel after different immersion periods, it is seen that only one semicircle is shown and its diameter increases with increasing the immersion time from 60 min to 210min. Polarization resistance increases with the immersion time, but if it reached 150 min, the charge transfer resistance (**Table 4**) value is substantially constant, this behavior is due to the gradual formation of the film due to the corrosion product of this type of steel. However, in the absence

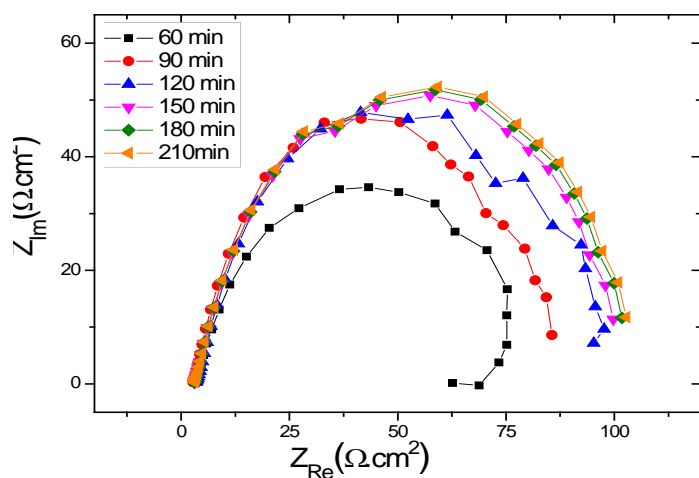


Figure 4. Nyquist plots obtained for X70 steel sample after different immersion times in 3% NaCl solutions at room temperature

Table 4. EIS parameters of X70 steel sample after different immersion times in 3% NaCl solutions at room temperature

Immersion Times (min)	60	90	120	150	180	210
R_{ct} (Ω/cm^2)	74.2	86.8	101.3	105.9	104.6	105.4
C_{dc} (mF/cm^2)	2.784	2.534	2.221	1.984	1.865	1.965

of inhibitors, the polarization resistance value is minimal and does not allow a proper protection of steel.

The charge transfer resistance, R_{ct} values are calculated from the difference in impedance at lower and higher frequencies, as suggested by Tsusu and Haruyama [17]. The correction in the capacitance to its real value is calculated using the relation (5) [18].

$$f(-Z_{max}) = \frac{1}{2\pi C_{dc} R_{ct}} \quad (5)$$

The inhibition efficiency IE (%) was calculated using the charge transfer resistance as follows:

$$\text{IE}(\%) = \frac{(R'_{ct} - R_{ct})}{R'_{ct}} \times 100 \quad (6)$$

where R_{ct} and R'_{ct} are the charge transfer resistance in the absence and presence of inhibitor, respectively.

Nyquist impedance plots for the same experimental conditions are shown in **Figure 5**.

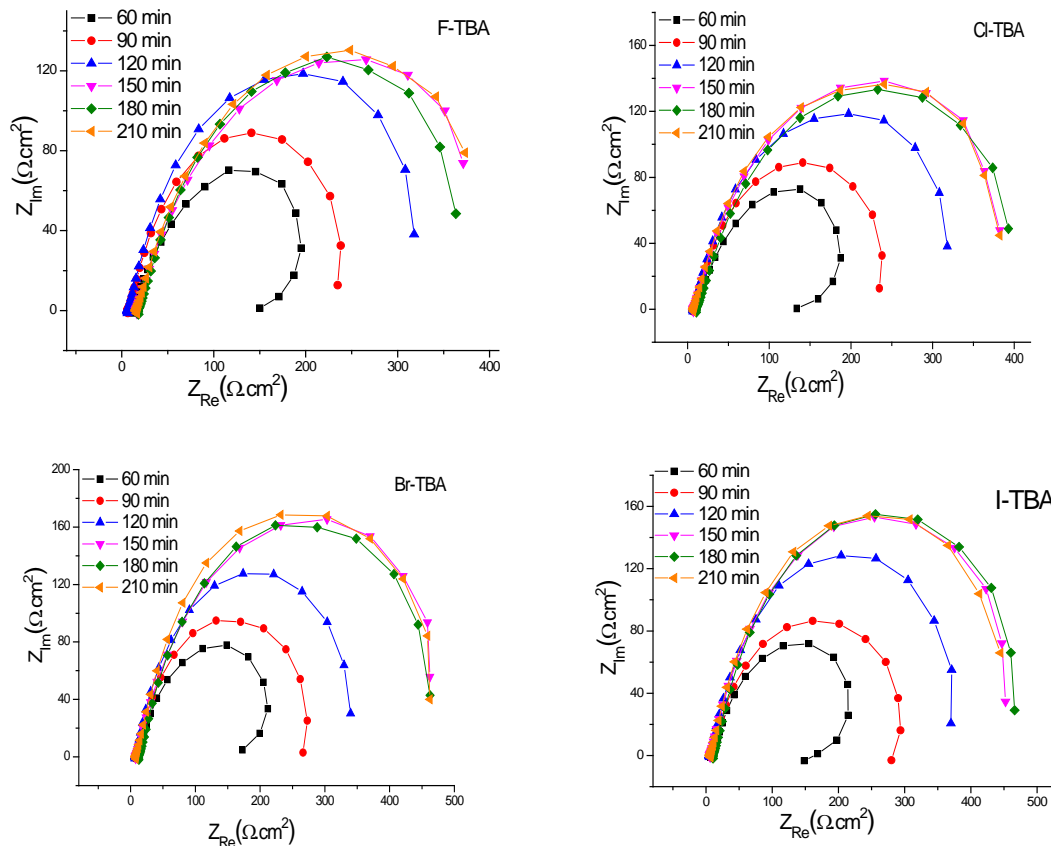


Figure 5. Nyquist diagrams of X70 steel electrode in 3%NaCl + 10^{-3} M of X-TBA at E_{corr}

The Nyquist plots for X70 steel have the form of depressed semicircles with the center under the real axis. The depressed semicircle form is characteristic of dispersion in frequency and has been attributed to different physical phenomena such as roughness and inhomogeneities of solid surfaces during corrosion [19]. Increase in the diameters of the semicircles with the concentration of X-TBA indicates that there is an increase of protective properties of the steels surface. Thus, the capacitive semicircle is correlated with the dielectric properties and the thickness of adsorbed film.

The result suggests a passive state associated with the formation of a film inhibitor (semicircle at high frequency) while the low frequency semicircle charges transfer processes that are the salt of the film at local sites [20-22].

Table 5. Polarization resistance and inhibition efficiency of X70 steel in 3%NaCl + 10⁻³M of X-TBA

Immersion times (min)	R _{ct} (Ω/cm ²)					Efficiencies %			
	Blank	F-TBA	Cl-TBA	Br-TBA	I-TBA	F-TBA	Cl-TBA	Br-TBA	I-TBA
60	74.2	222.8	236.2	255.4	272.6	66.70	68.59	70.95	72.78
90	86.8	265.9	283.1	298.1	305.1	67.36	69.34	70.88	71.55
120	101.3	355.5	369.2	397.3	409.6	71.50	72.56	74.50	75.27
150	105.9	396.1	410.4	485.8	506.4	73.52	74.44	78.41	79.29
180	104.6	401.2	408.7	474.1	518.3	73.87	74.16	77.73	79.63
210	105.4	402.6	411.4	488.4	512.7	74.20	74.38	78.42	79.44

CONCLUSION

Following the above conducted studies, broad conclusions were drawn; the X70 steel is not resistant for corrosion in 3% NaCl and at low acidity. Polarization resistance increases with immersion time until an optimal time of 150 min due to the formation of a protective film. Comparison between the investigated inhibitors reveals that I-TBA is the most efficient one due to its high IE% (78–79%) that was obtained at relatively low concentration. The adsorption on X-70 steel surface by inhibitors molecules, obey Langmuir isotherm, the adsorption is a spontaneous endothermic process. According to the values of free energy of adsorption obtained we recommend the Physical adsorption process.

REFERENCES

1. McCafferty, E. & Hackerman, N. (1972). Kinetics of iron corrosion in concentrated acidic chloride solutions. *J Electrochem Soc*, 119, 999.
2. Kaesche, H., & Hackerman, N. (1958). Corrosion Inhibition by Organic Amines. *J Electrochem Soc*, 105, 191.
3. Soror, T. Y., & El-Ziady, M. A. (2002). Effect of cetyl trimethyl ammonium bromide on the corrosion of carbon steel in acids. *Materials Chemistry and Physics*, 77, 697.
4. Ali, S. A., & Saeed, M. T. (2001). Synthesis and corrosion inhibition study of some 1,6-hexanediamine-based N,N-diallyl quaternary ammonium salts and their polymers. *Polymer*, 42, 2785.
5. Vasudevan, T., Muralidharan, S., Alwarappan, S., & Iyer, S. V. K. (1995). The influence of N-hexadecyl benzyl dimethyl ammonium chloride on the corrosion of mild steel in acids *Corros. Sci*, 37, 1235.
6. Hamdi, A., Taouti, M. B., & Benbertal, D. (2015). Corrosion inhibition of X70 steel by thiourea-Zinc thiocyanate system in sodium chloride solution. *J. Mater. Environ. Sci* 6, 93.
7. Ferhat, M., Benchettara, A., & Asma, S. E. (2014). Effect of copper on passivity and corrosion behavior of Fe-xC-5Cu alloy. *J. Fund. App. Sci*, 6, 94.
8. Kadiri, C., Mokhtar, S., Benbertal, D., & Ameer, K. (2006). *J. Saudi Chem. Soc.*, 10, 549-561
9. Dermaja, A., Hajjaji, N., Joiret, S., Rahmouni, K., Srhiri, A., Takenoutia, H. & Viviera, V. (2007). Electrochemical and spectroscopic evidences of corrosion inhibition of bronze by a triazole derivative. *Electrochimica Acta*, 52, 4654.
10. Schweinsberg, D. P., & Ashworth, V. (1988). The inhibition of the corrosion of pure iron in 0.5 M sulphuric acid by n-alkyl quaternary ammonium iodides. *Corros. Sci*, 28, 539.
11. Maghraby, A. A., & Soror, T. Y. (2010). Quaternary ammonium salt as effective corrosion inhibitor for carbon steel dissolution in sulphuric acid media. *Advances in Applied Science Research*, 1, 143.

12. Niu, L., Zhang, H., Wei, F., Wu, S., Coa, X., & Liu, P. (2005). Corrosion inhibition of iron in acidic solutions by alkyl quaternary ammonium halides: Correlation between inhibition efficiency and molecular structure. *Applied Surface Science*, 252, 1634.
13. Xianghong, L., Shuduan, D., Hui, F., Taohong, L. (2009). Adsorption and inhibition effect of 6-benzylaminopurine on cold rolled steel in 1.0 M HCl. *Electrochimica Acta*, 54, 4089.
14. Keles, H., Keles, M., Dehri, I., & Serindag, O. (2008) The inhibitive effect of 6-amino-m-cresol and its Schiff base on the corrosion of mild steel in 0.5M HCl medium. *Mater. Chem. Phys*, 112, 173.
15. Alberty, R., & Silbey, R. (1997). *Physical Chemistry*, second ed, Wiley, New York, USA, pp. 845.
16. Schapink, F. W., Oudeman, M., Leu, K. W., & Helle, J. N. (1960). The adsorption of thiourea at a mercury-electrolyte interface. *Transactions of the Faraday Society*, 56, 415.
17. Tsuru, T., Haruyama, S., & Gijutsu, B. (1978). Corrosion inhibition of iron by amphoteric surfactants in 2M HCl. *J Japan Soc Corros Eng*, 27, 573.
18. Machnikova, E., Kenton, W. H., & Hackerman, N. (2008). Corrosion inhibition of carbon steel in hydrochloric acid by furan derivatives. *Electrochim Acta*, 53, 6024.
19. Jüttner, K. (1990). Electrochemical impedance spectroscopy (EIS) of corrosion processes on inhomogeneous surfaces. *Electrochim Acta*, 35, 1501.
20. Digby, D., & Macdonald. (1978). A Method for Estimating Impedance Parameters for Electrochemical Systems That Exhibit Pseudoinductance. *Electrochem. Soc*, 125, 2062.
21. Khaled, K. F. (2010). Understanding Corrosion Inhibition of Mild Steel in Acid Medium by Some Furan Derivatives: A Comprehensive Overview. *J. Electrochem. Soc*, 157, 116.
22. Zarrouk, A., Zarrok, H., Salghi, R., Hammouti, B., Bentiss, F., Touir, R., & Bouachrine, M. J. (2013). Evaluation of N-containing organic compound as corrosion inhibitor for carbon steel in phosphoric acid. *Mater. Environ. Sci*, 4, 177.

<http://www.eurasianjournals.com>